Modal-based structural damage identification by minimum constitutive relation error and sparse regularization

Jia Guo[1,3], Li Wang[*,2], and Izuru Takewaki[1]

[1]Department of architecture and architectural engineering, Kyoto University, Kyoto, Japan

[2]Department of applied mechanics and engineering, Sun Yat-sen University, Guangzhou, P.R. China

[3]Research institute of highway, Ministry of Transport, Beijing, 100084, P.R. China

Abstract

This paper presents a novel sparse-regularized minimum constitutive relation error (min-CRE) approach for structural damage identification with modal data. In this approach, the inverse identification problem is treated as a nonlinear optimization problem whose objective function is just the constitutive relation error (CRE). To circumvent the ill-posedness of the inverse problem which is caused by use of the possibly insufficient modal data and enhance the robustness of the identification process, a sparse regularization is introduced where a sparse (or ℓ_1-norm) regularization term is added to the original CRE function. In regard to the minimum solution of the sparse-regularized CRE objective function, a two-step substitution algorithm is established. The attractive feature of the present damage identification approach is that no sensitivity analysis is involved herein and the additional introduction of the sparse regularization term introduces little computational complexity. The approach is applied to damage identification of one or two-dimensional beam structures with experimental or simulated modal data. Results show that the sparse regularization indeed improves the effectiveness and robustness of the min-CRE approach under measurement noises and initial model errors, even in the case of large damages.

Keywords: damage identification, constitutive relation error(CRE), sparse regularization, incomplete modal data, ill-posedness

*Correspondence to: Li Wang, Email: wangli75@mail.sysu.edu.cn

1 Introduction

One of the main issues to be confronted with in structural engineering, is identification of the damages. Due to the convenience in modal data, e.g., through ambient tests, a great deal of modal-based methods have been developed to detect the structural damages[1]. These methods are all based on the fact that damages, often embodied as degradation of structural stiffness, would introduce changes into the dynamic characteristics such as frequencies and modal displacements.

In fact, the modal-based damage identification methods are mainly categorized into two classes. In the first class, damages are directly identified from the change in the modal strain energy[2-4]. However, this kind of methods is often noise sensitive[5]. Sensitivity-based approaches are fallen into the second class[6-8]. They treat the damage identification problem as a nonlinear optimization problem, for which the objective function is posed to be the weighted least-squares of the errors between the measured modal data and the derived data, and sensitivity analysis is invoked in order to solve the nonlinear optimization problem. The sensitivity-based approaches are now widely used in structural damage identification.

Recently, the idea of using an error in constitutive relation for structural damage identification has caught the attention of researchers; it leads to the minimum constitutive relation error (min-CRE) approach. The approach treats the damage identification problem as a nonlinear optimization problem and its objective function is selected as the constitutive relation error (CRE), that is, energy inner product of the residual of the constitutive equations connecting between the admissible stresses and the kinematically admissible displacements. One attractive feature of the min-CRE approach is that the objective function is (separately) convex, for which only first-order conditions are sufficient conditions for optimality and the global minimum is always reached. Moreover, the sensitivity analysis which constitutes the main part of the computational cost for the sensitivity-based approaches is no longer needed, rather, a simple two-step substitution algorithm is often called to solve this minimization problem[9-11]. Actually, this min-CRE approach was first proposed for model updating analysis, using full-field static displacement data in linear elasticity[12]. Then the approach was extended to tackle many other damage parameter identification problems: in linear statics beam structure[13], transient dynamics[14], elastoplastics[15] and so on[16;17].

The main difficulty in applying the min-CRE approach resides at the admissible stress field for 2D or 3D problems which has to be built a priori before the min-CRE process. Fortunately, for conventional beam structures, the force method can be utilized to get the admissible stress

field. A noteworthy thing for the damage identification problem is that compared to the infinite number of modes for a continuous structure, incomplete measured modal data is always available in experimental testing due to limitations of sensor number, excitation imperfection, etc. The insufficient amount of the measured data could make the damage identification problem ill-posed and very sensitive to the measurement noise. To circumvent this drawback, regularization techniques such as the Tikhonov regularization and the sparse (or ℓ_1-norm) regularization need to be introduced[18;19]. The idea that all the damages or changes of parameters are as small as possible is implicated in the Tikhonov regularization. Such an idea is reasonable for finite element updating, but may not be appropriate for damage identification since large damages may occur[20;21]. For practical structures, the amount of the (small or large) damages is often scarce and this, in principle, shall be well implicated in the sparse regularization[22]. As a consequence, the sparse regularization is often preferred for the structural damage identification. Part of the earliest contributions to the damage identification based on the sparse regularization have been extensively studied in Refs.[23;24] where sparse representation classification using mode shapes was proposed. The physical interpretation of sparse regularization with A_1-norm as the sparse location of sensors in structures was also addressed in Refs.[25;26].

Above all, this paper is focused on the structural damage identification with (incomplete displacement) modal data by the min-CRE approach and the sparse regularization. In the proposed method, several attractive features are expected to be reached; they are

1. The objective function is separately convex and therefore, large damages may become identifiable.

2. The sparse regularization is enforced such that insufficient or incomplete modal data can also lead to good identification.

3. The regularization parameter is automatically selected with a computationally simple and effective strategy.

4. Though the sparse regularization has already been incorporated into the sensitivity-based approaches[20;27;28], the incorporation is not straightforward at all, because minimization of the linearized objective function along with the sparse regularization term at every sensitivity-based iteration should again resort to an iterative procedure. In contrast, minimization of the CRE objective function along with the sparse regularization over the damage parameters can be directly solved at once with closed-form solutions. Moreover, no sensitivity analysis needs to be called in the present sparse-regularized min-CRE ap-

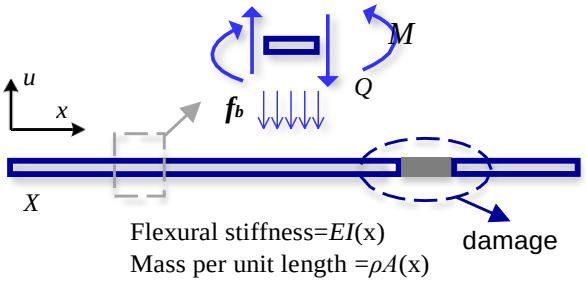

Figure 1 Model of Euler-Bernoulli beam

proach and the exact order, e.g., 1st/2nd of the mode shape which must be known in the sensitivity-based approaches, is not required in the min-CRE approach.

The remainder of this paper is organized as follows. The basic inverse identification problem with the min-CRE objective function is briefly introduced in Section 2. In Section 3, the sparse regularization is applied to enhance the CRE objective function and then, a two-step substitution algorithm is presented to get the solution. Numerical tests and experimental verification are performed in Sections 4 and 5 and final conclusions are drawn in Section 6. For the convenience of presentation, one and two-dimensional problems are discussed in this research. The extension of the basic methodology to multi-dimension problem would be straightforward.

2 Problem statement

2.1 The baseline model

Consider an Euler-Bernoulli beam occupying the physical domain $x \in X$. Let $(u_i(x),\ \theta_i(x))$ denote the deflection and rotation of the ith mode shape and $M_i(x)$, $Q_i(x)$ the corresponding bending moment and shear force. The flexural stiffness and mass per unit length are denoted by EI and ρA as shown in **Figure 1**. The support displacements satisfy the homogeneous Dirichlet boundary conditions, or mathematically $u_i(x) \in \mathcal{U}_0$, $\mathcal{U}_0 = \{u_i \in H^2(X) : u_i$ satisfy the homogeneous Dirichlet boundary conditions$\}$ and $(M_i(x), Q_i(x))$ satisfy the homogeneous Neumann boundary conditions, or mathematically $M_i(x) \in \mathfrak{I}_0$, $\mathfrak{I}_0 = \{M_i'' \in L^2(X) : M_i$ satisfy the homogeneous Neumann boundary conditions$\}$. As is noteworthy, H^2 is the Sobolev space defined with the derivatives up to the second order being square-integrable and it is usually known as containing the C^1-continuous functions and L^2 is the Lebesgue space of square-integrable functions. With these notations, the free vibration of the Euler-Bernoulli beam is divided into three parts.

· **Kinematic constraints**

$$u_i(x) \in \mathcal{U}_0 \tag{1}$$

· **Equilibrium equations**

$$f_{bi}(x) + M_i''(x) = 0 \tag{2}$$

where $f_{bi}(x)$ is the transversal inertial force per unit length and $M_i(x) \in \mathfrak{I}_0$. Moreover, the equilibrium equations as well as the boundary conditions (by principle of virtual work) could also be expressed as

$$\int_x f_{bi}(x)\delta u_i \, dx + \int_x M_i(x)\delta u_i'' \, dx = 0, \forall \delta u_i \in \mathcal{U}_0 \tag{3}$$

· **Constitutive relations**

$$M_i(x) = EIu_i''(x) \text{—Hooke's law,} \tag{4a}$$

$$f_{bi}(x) = \rho A\ddot{u}_i(x) \text{—Newton's law.} \tag{4b}$$

By the use of the relations $\ddot{u}_i(x) = -\omega_i^2 u_i(x)$ in free vibration analysis, where ω_i is the ith natural frequency, equation (4b) could be simplified as $f_{bi}(x) = -\omega_i^2 \rho A u_i(x)$.

2.2 CRE function for a given mode

To define the constitutive relation error for the ith mode shape, consider an admissible displacement solution $\mathcal{W}_i = u_i(x) \in \mathcal{U}_0$, an admissible force solution $\mathcal{F}_i = M_i(x) \in \mathfrak{I}_0$ which satisfies equilibrium equations (2) and the admissible structural parameters $\mathcal{K} \in \mathcal{C}$ which may include some model's parameters such as Young's modulus, mass density and cross-section information of the beam. It is easily known that, if the constitutive relation (4) is additionally satisfied, the above solution would be the exact eigenmodes of this structure.

As a result, to measure the distance of the admissible solutions to the exact solutions in the energy product, the constitutive relation error for the ith mode of the beam is defined by

$$e_{CRE}(\mathcal{W}_i, \mathcal{F}_i, \mathcal{K}) = \frac{r}{2}\int_X \frac{(M_i - EIu_i'')^2}{EI} dx + \frac{1-r}{2}\int_X \frac{\left(f_{bi} + \omega_i^2 \rho A u_i\right)^2}{\omega_i^2 \rho A} dx \tag{5}$$

where $r \in [0, 1]$ is the corresponding weight which depends on the relative reliability between the constitutive relation (4) based on the Hooke's law and based on the Newton's law and is fixed to be $r = 0.5$ in this paper.

For this free vibration problem, further considering the equilibrium equations (2), the CRE in (5) could be simplified into:

$$e_{CRE}(\mathcal{W}_i, \mathcal{F}_i, \mathcal{K}) = \frac{r}{2}\int_X \frac{(M_i - EIu_i'')^2}{EI} dx + \frac{1-r}{2}\int_X \frac{\left(M_i'' - \omega_i^2 \rho A u_i\right)^2}{\omega_i^2 \rho A} dx \tag{6}$$

Then the parameter identification formulation based on the given complete mode data u_i is established as:

$$F_i(\mathcal{W}_i, \mathcal{F}_i, \mathcal{K}) := e_{CRE}(\mathcal{W}_i, \mathcal{F}_i, \mathcal{K})$$
$$(\mathcal{F}_i, \mathcal{K}) = \arg \min_{\mathcal{F}_i \in \mathfrak{F}_0, \mathcal{K} \in \mathcal{C}} F_i(\mathcal{W}_i, \mathcal{F}_i, \mathcal{K}) \quad (7)$$

which is known as the min-CRE principle for inverse identification problems[12] and $F_i(\mathcal{W}_i, \mathcal{F}_i, \mathcal{K})$ is known as the objective function.

In many situations, the complete or full-field mode data u_i is often hardly available, rather, the incomplete modal displacement data measured by finite sensors is obtained. Herein, an additional penalty term is incorporated into the constitutive relation error function (7) in order to simply enforce the conditions of the measured data. Such a penalty term can also account for the different level of reliability or measurement noise of the experimental measurement data. More specially, the objective function for damage identification using the ith mode data is modified as follows

$$\widehat{F}_i(\mathcal{W}_i, \mathcal{F}_i, \mathcal{K}) := e_{CRE}(\mathcal{W}_i, \mathcal{F}_i, \mathcal{K}) + \sum_{k \in \wp} \frac{A_k}{2} |u_{ki} - \hat{u}_{ki}|^2 \quad (8)$$

where $\{\hat{u}_{ki}, k \in \wp\}$ is the measured displacement modal data on the set of points $\{k \in \wp\}$ and u_{ki} is the admissible modal displacement at kth position for the ith mode. Values of $\{A_k > 0, k \in \wp\}$ could be tuned according to the confidence of the corresponding displacement data: $\{A_k \to +\infty\}$ means completely trust of this data, while $\{A_k \to 0\}$ means completely untrust.

2.3 CRE function for multiple modes

In order to identify the damage parameters, multiple modal data $\{(u_{ki}, \omega_i), i \in S\, k \in \wp\}$ are often measured, where S denotes the set of all modal data. The objective function (CRE function) for multiple modes is defined as follows

$$F(\mathcal{W}, \mathcal{F}, \mathcal{K}) = \sum_{i \in S} t_i \widehat{F}_i(\mathcal{W}_i, \mathcal{F}_i, \mathcal{K}) = \sum_{i \in S} t_i \left(e_{CRE}(\mathcal{W}_i, \mathcal{F}_i, \mathcal{K}) + \sum_{k \in \wp} \frac{A_k}{2} |u_{ki} - \hat{u}_{ki}|^2 \right) \quad (9)$$

where t_i is the corresponding weight coefficient and $\mathcal{W} = \{\mathcal{W}_i, i \in S\}$, $\mathcal{F} = \{\mathcal{F}_i, i \in S\}$. Herein, the weight coefficient t_i should be chosen based on the reliability of each mode.

3 Damage identification by min-CRE and sparse regularization

Section 2 presents the basic background of the min-CRE principle for beam structures. In practice, the amount of the measured modal data is always limited and this may make the damage

identification problem ill-posed. To properly circumvent the ill-posedness, the sparse regularization technique is reasonably introduced and a two-step substitution algorithm is proposed to practically solve the nonlinear optimization problem in this section. Particular attention is paid to estimation of the regularization parameters for the sparse regularization.

3.1 Solution by two-step substitution algorithm

- step 1 (UMF Step): Update the Mechanical Field $(\mathcal{W}_i, \mathcal{F}_i)$ for the ith mode with the given material parameters $\mathcal{K}^n$

$$\left(\mathcal{W}_i^{n+1}, \mathcal{F}_i^{n+1}\right) = \arg \min_{\mathcal{W}\in\mathcal{U}_0, \mathcal{F}\in\Im_0} \widehat{F}\left(\mathcal{W}_i, \mathcal{F}_i, \mathcal{K}^n\right), i \in S \tag{10}$$

- step 2 (UMP Step): Update the Material Parameters $\mathcal{K}$ by the mechanical fields $\left(\mathcal{W}_i^{n+1}, \mathcal{F}_i^{n+1}\right)$ obtained in step 1.

$$\mathcal{K}^{n+1} = \arg\min F\left(\mathcal{W}^{n+1}, \mathcal{F}^{n+1}, \mathcal{K}\right) = \arg \min_{\mathcal{K}\in\mathcal{C}} \sum_{i\in S} t_i \widehat{F}\left(\mathcal{W}_i{}^{n+1}, \mathcal{F}_i{}^{n+1}, \mathcal{K}\right) \tag{11}$$

3.2 The UMF Step

The mechanical field $(\mathcal{W}_i, \mathcal{F}_i)$ is recovered from the measured data and the given material parameters $\mathcal{K}$ individually for every mode. The sparse regularization term is not involved in this step. Specifically, the minimization over $\mathcal{F}_i$ yields the equation:

$$\int_x \left\{ r\frac{\delta M_i M_i}{EI} + (1-r)\frac{\delta M_i{}'' M_i{}''}{\omega_i^2 \rho A} - \delta M_i{}'' u_i \right\} dx = 0, \forall \delta M_i \in \Im_0 \tag{12}$$

and the minimization over $\mathcal{W}_i$ yields

$$\int_x \{ rEI\delta u_i{}'' u_i{}'' + (1-r)\omega_i^2 \rho A \delta u_i u_i - \delta u_i M_i{}'' \} dx + \sum_{k\in\wp} A_i \delta u_{ki} |u_{ki} - \hat{u}_{ki}| = 0, \forall \delta u_i \in \mathcal{U}_0 \tag{13}$$

From equations (12) and (13), the mechanical field $(\mathcal{W}_i, \mathcal{F}_i)$ can be updated simultaneously. Practically, equations (12) and (13) are dealt with in the finite element setting and the detailed procedure is given in Appendix.

3.3 The UMP Step

The damage parameters for the Euler-Bernoulli beam structure in this paper is set to be $\mathcal{K} = EI(x)$ and, the sparse regularization term is involved and needs to be properly tackled. The sparsity assumption that the number of damage locations of a structure is as few as possible is sensible for the practical damage identification problem. Properly enforcing the sparsity

assumption could improve the robustness of the identification results[21] and this shall be easily reached by the sparsity regularization technique.

Assume that the stiffness EI is piecewise constant, that is to say $EI(x) = \{EI_p, x \in X_p, p = 1, 2, \ldots, N\}$, where $\{X_p, p = 1, 2, \ldots, N\}$ is the non-overlapping decomposition of the whole domain X. Then, with the sparse regularization, the objective function is reformulated as

$$\sum_{i\in S}\int_{X_p} t_i \left\{\frac{r}{2}\frac{\left(M_i - EI_p u_i''\right)^2}{EI_p} + \frac{1-r}{2}\frac{\left(M_i'' - \omega_i^2 \rho A u_i\right)^2}{\omega_i^2 \rho A}\right\} dx + \lambda l_p \left\|EI_p - EI_{0p}\right\|_1^1, p = 1,2,\ldots,N \qquad (14)$$

where $\{l_p, p = 1, 2, \ldots, N\}$ is the length of EI_p and EI_{0p} is set to be the stiffness of the structure before damaged. $\left\|EI_p - EI_{0p}\right\|_1^1$ is the sparse regularization term with $\|x\|_1 = |x|$ being the ℓ_1-norm. $\lambda > 0$ is the regularization parameter which controls the trade-off between the sparsity and the residual norm. It has been proved that minimization of ℓ_1-norm could satisfy the desired sparsity requirement[22]. Moreover, $\|x\|_1$ is still convex and the linear programming techniques[22] can be easily called to solve the optimization problem in the conventional linear least squares setting. Thus, in this paper, the choice ℓ_1-norm is fixed. Furthermore, the partial differential equation of equation (14) for $\{EI_p, x \in X_p, p = 1, 2, \ldots, N\}$ takes the form

$$\frac{\partial L_1}{\partial EI} = \sum_{i\in S}\int_{X_p} t_i r \left\{\frac{{M_i}^2}{{EI_p}^2} - (u_i'')^2\right\} dx - \lambda l_p \{\mathrm{sign}(EI_p - EI_{0p})\} dx = 0 \qquad (15)$$

Finally, one has

$$\mathrm{E}I_p = \begin{cases} \sqrt{\frac{b_p}{a_p + \lambda l_p}}, \text{if } \lambda < \Lambda_p \\ \sqrt{\frac{b_p}{a_p - \lambda l_p}}, \text{if } \lambda < -\Lambda_p \\ \mathrm{E}I_{0p}, \text{ if } \lambda \geq |\Lambda_p| \end{cases}, p = 1,2,\ldots,N \qquad (16)$$

where

$$\Lambda_p = \frac{1}{l_p}\sum_i \int_{X_p} t_i r \left\{\frac{{M_i}^2}{{EI_{0p}}^2} - (u_i'')^2\right\} dx = \frac{1}{l_p}\left(\frac{b_p}{EI_{0p}^2} - a_p\right) \qquad (17)$$

and

$$a_p = \sum_i \int_{X_p} t_i r (u_i'')^2 \, dx, \; b_p = \sum_i \int_{X_p} t_i r {M_i}^2 \, dx \qquad (18)$$

Datailed explanations of Λ_p are discussed in the next section. From equations (15) and (16), the sparse regularization term would introduce little computational complexity and the minimization over the damage parameters along with the sparse regularization term is solved immediately by the closed-form solution in equation (16) for the sparse-regularized min-CRE

approach. However, in the sensitivity-based approaches[21], the sparse regularization term in each sensitivity step must be dealt with in a costly manner by iterative algorithms, e.g., the

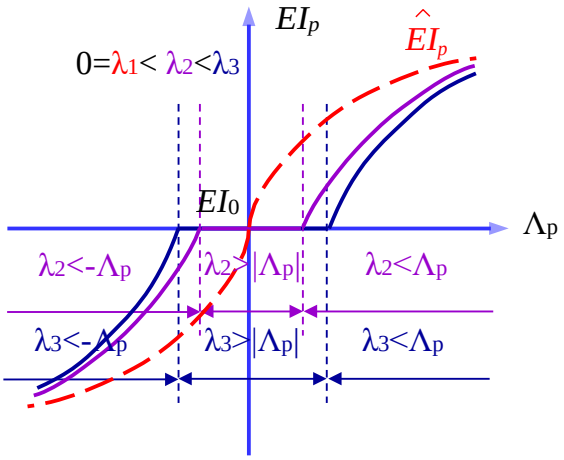

Figure 2 Sparsity with different values of λ

linear programming method or the interior point method. Moreover, no sensitivity analysis is involved in the proposed approach. All these have constituted the advantages of the proposed min-CRE approach over the conventional sensitivity-based approaches.

To get a better perspective of equation (16) and the sparsity-promoting nature of ℓ_1-norm regularization, $\hat{EI}_p$ (dotted line in **Figure 2**) is introduced for the situation when no sparsity is considered (λ = 0)

$$\hat{EI}_p = \sqrt{\frac{\sum_i \int_{x_p} t_i M_i^{\,2}\, dx}{\sum_i \int_{x_p} t_i (u_i'')^2\, dx}} = \sqrt{\frac{b_p}{a_p}}, p = 1,2,\dots,N \tag{19}$$

Based on equations (16) and (19), **Figure 2** illustrates the relationship between EI_p and $\hat{EI}_p$ with different values of λ. **Figure 2** shows that the value of EI_p is prone to be unchanged from the initial value EI_{0p} when $\lambda \geq |\Lambda_p|$ while EI_p begins to deviate from EI_{0p} to $\hat{EI}_p$ when $\lambda < |\Lambda_p|$. That is to say, the regularization parameter λ determines whether damage occurs: as long as $\lambda < |\Lambda_p|$, the pth element would admit stiffness change or damage; otherwise if $\lambda \geq |\Lambda_p|$, the damage would be found to not occur in the pth element.

3.4 Regularization Parameter Estimation

As shown in many Refs.[29;30], the regularization parameter λ plays an important role in the quality of the damage identification results, especially in cases where high levels of noise are present in the data. In this section, a novel and simple strategy, named "threshold setting method", for estimating the optimal regularization parameter λ_{est}, is devised.

For each iterative step, $\{|\Lambda_p|, p = 1,2,\dots,N\}$ could be obtained for each element by equation (17). From **Figure 2**, one could see a close relationship between λ and $\{|\Lambda_p|,\ p = 1,2,\dots,N\}$.

In fact, λ is used to distinguish the damaged elements from the undamaged elements and $|\Lambda_p|$ reflects the difference between the stiffness obtained directly from the CRE objective function without sparsity ($\hat{EI}_p$) and the undamaged stiffness (EI_{0p}) for each element. It is easily known that if this difference is large enough ($|\Lambda_p| > \lambda$), damage is reasonably assumed to occur. In other words, elements with higher values of $|\Lambda_p|$ are likely to be damaged with stronger possibility while lower values indicate undamage and perturbation errors. Thus, setting one of the values in $\{|\Lambda_p|\ , p = 1, 2, \ldots, N\}$ as threshold could separate the damaged and undamaged elements.

As a result, a simple procedure to estimate the optimal regularization parameter λ_{est} is proposed for each iterative step as follows:

1. Get $\{|\Lambda_p|\ , p = 1, 2, \ldots, N\}$ from equation (17) and sort the absolute values in descending order, leading to $\{\hat{\Lambda}_1 \geq \hat{\Lambda}_2 \geq \ldots\}$;

2. Fix the maximum threshold setting rank $l_{\max}$ and the discriminating ratio α;

3. Obtain the optimal regularization parameter λ_{est}: for each $l = 1, \ldots, l_{\max} - 1$,

$$\lambda_{\text{est}} = \begin{cases} \hat{\Lambda}_{l+1}, & \text{if } \hat{\Lambda}_l \geq \alpha \hat{\Lambda}_{l+1} \\ \hat{\Lambda}_{l_{\max}}, & \text{else} \end{cases} \tag{20}$$

The maximum threshold setting rank $l_{\max}$ limits the maximum number of possible damages and principally one tends to choose a relatively small value of $l_{\max}$ to guarantee the sparsity of the identification results. On the other hand, it is conceivable that the general undamaged elements have relatively small values of $|\Lambda_p|$ corresponding to the noise level and would be quite away from $|\Lambda_p|$ of the damaged elements. As a result, the discrimination ratio α measures the distance between the minimum error caused by possible damages and the maximum error purely invoked by the measurement noise level. If $\hat{\Lambda}_l$ is much greater than $\hat{\Lambda}_{l+1}$ ($\hat{\Lambda}_l \geq \alpha \cdot \hat{\Lambda}_{l+1}$), element l is identified as damaged. The maximum threshold setting rank $l_{\max}$ gives possible maximum number (initial guess) of damages while the discrimination ratio α narrow it down. The choice of α should be very careful in the multiple damage case because it directly affects the identified number of damages. Nevertheless, the identification process tends to be reasonably robust with a broad selection of α, which will be illustrated in detail in the later numerical example. In this paper, $l_{\max} = 5$ and an empirical value $\alpha = 4$ is used.

4 Numerical simulation

In the following, several numerical simulations are used to test the proposed sparse-regularized

min-CRE approach. The performance of the threshold setting method to give the regularization

parameter and the effectiveness and superior identifiability for structures with different damage severities by the sparse-regularized min-CRE approach are demonstrated in sections 4.1 and 4.2. Section 4.3 shows that the sparse regularization can significantly improve the robustness of the identification results from Monte Carlo simulations.

4.1 A two-span continuous beam with single and multiple damage cases

A numerical equi-spaced two-span continuous beam was studied to test the proposed threshold setting method at first. The first three modal responses of this beam were generated using finite element software. For detailed information on the geometry and boundary of the structure as well as the specific enumeration of the 17 equidistant measurement points, refer to **Figure 3**. 64 Euler-Bernoulli beam elements were used both for the modal evaluation model and the identification model. Damages were enforced by reducing the stiffness of the corresponding elements. Two damage cases are taken into account, including:

- Single damage case D1: stiffness reduced to 50% in element 21; and
- Multiple damage case D2: stiffness reduced to 90%, 80% and 85% in elements 16, 22 and 46 respectively.

Figure 4 shows the identification results in cases D1 and D2, using the proposed sparse-regularized min-CRE approach with threshold setting method to select the optimal regularization parameter λ_{est}. Noise is not considered herein. Good identification performance for this two-span continuous beam structure is achieved. The optimal regularization parameter λ_{est} from the threshold setting method in Section3.4 is 6.57×10^{-06} for D1 and 1.84×10^{-04} for D2 for the convergence step.

Next, to have an impression on how the regularization parameter λ affects the identification results in the min-CRE approach and testify the efficiency of the threshold setting method, changes in EI with different regularization parameters λ are additionally plotted in **Figure 5** for both single damage case D1 and multiple damage case D2. As is observed, smaller value of λ or say, weaker enforcement of sparsity renders the identified results more sensitive to the error and uncertainty in modeling and simulation while very large value of λ or stronger enforcement of sparsity may fail in identifying damages or produce biased damage extents. **Figure 5** shows that $\lambda \in [10^{-6}, 10^{-3}]$ in D1 and $\lambda \in [10^{-4}, 10^{-3}]$ in D2 could result in satisfactory identified results, coinciding well with the good identification results from the threshold setting method as in **Figure 4** and again verifying the effectiveness of the threshold setting method. In addition,

Figure 5 exhibits a broader selection of λ in the single damage case D1 than in the multiple damage case D2. The choose of the regularization parameter λ must be paid more attention for multiple damage cases consequently.

To testify the robustness of the threshold setting method, a normal distribution noise is added to the simulated modal response as

$$\text{noise}(x) = randn \cdot a \cdot \varphi(x) \tag{21}$$

where *randn* is the normal distribution with zero mean and unit deviation, a is the applied noise level and $\varphi(x)$ is the measured modal displacements at a certain point x. Noises of level 3% (Signal-to-Noise-Ratio, SNR=15dB) as well as 5% (SNR=13dB) for both of the cases D1 and D2 are considered in this example. As the natural frequencies can be often measured with negligible error compared with the mode shapes, noise for natural frequencies is not considered herein.

As shown in **Figure 6**, damages are identified successfully when the measurement noise is not greater than 5% in single damage case D1 with a value of $\lambda_{\text{est}} = 0.1644$. In contrast, multiple damage case D2 seems to be more sensitive to the noise: under 3% noise level, actual damages in elements 16, 22 and 46 were properly identified but unwanted yet acceptable stiffness change at element 55 was also observed (**Figure 6**(c)); while under 5% noise level, the actual damage in element 46 was missed but false positions near element 60 were observed (**Figure 6**(d)). This phenomenon is attributable to the different effectiveness of the sparse regularization. Single damage is apparently more in conformity with the sparsity assumption while multiple damages reduce sparsity in intensity and rely more on the data fidelity. Consequently, damages occurring at less locations achieve better identification results by the sparse-regularized min-CRE approach.

Figure 7 compares the evolution of CRE for each of the iterative step with different levels of noise. The error decreases with the number of iterations increases and most of the damages are identified after 30 steps, verifying the convergence of the present method.

To get a better picture on how the discriminating ratio α in the threshold setting method works when determining λ_{est}, further simulations are performed. Noise of level 3% for both of the cases D1 and D2 are considered herein. **Figure 8** shows the obtained optimal regularization parameter λ_{est} (in purple) with various values of the parameter α. As is expected, the choice of higher value of α may result in improper damage identification in the single damage case D1 while lower value of α leads to incomplete damage identification in the multiple damage case D2. The main reason for this observation lies in **Eq.** (20): larger value of α makes the condition

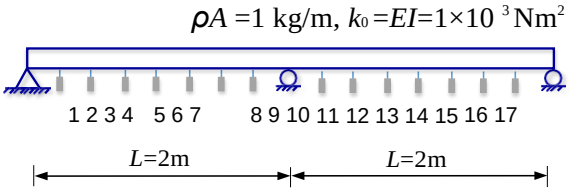

Figure 3 Model and measurement points of two-span continuous beam

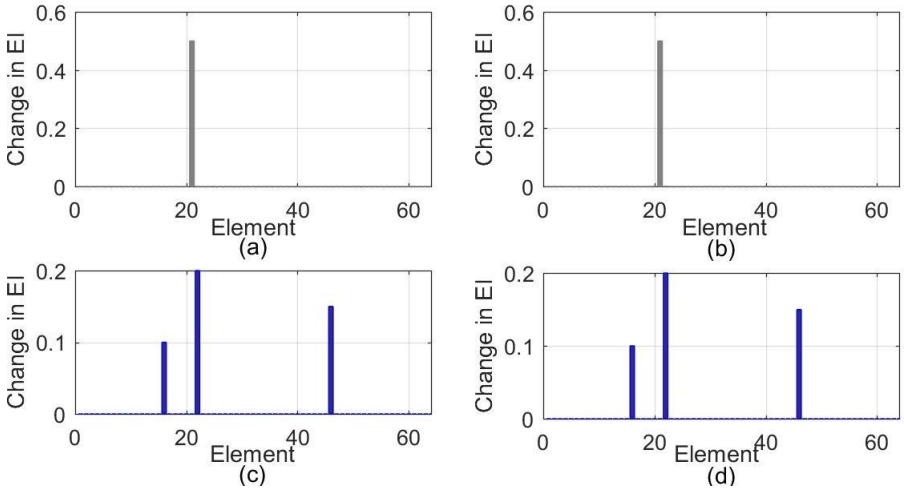

Figure 4 (a) actual damage for D1; (b) damage identification result for D1 using min-CRE approach with threshold setting method; (c) actual damage for D2; (d) damage identification result for D2 using min-CRE approach with threshold setting method

$\hat{\Lambda}_l \geq \alpha \cdot \hat{\Lambda}_{l+1}$ more difficult to be satisfied, implying that greater l is gained and less spare identification results are achieved. The appropriate ranges are $\alpha \in [1, 18]$ in D1 and $\alpha \in [3, 20]$ in D2. As is seen, the identification process is fairly robust for the choice of $\alpha \in [3, 18]$ and therefore, $\alpha = 4$ is used for the following examples in this paper.

4.2 Single cracked simply supported beams with different damage severity

Simply supported post-tensioned beams with different damage extents are to be identified in this example (see the Ref.[31] for details of the structure). Parameters of the simply supported beam are: length L = 3.6m, rectangular cross-section $t \times H$ = 0.1m × 0.125m, stiffness of the beam before damaged $k^0 = EI = 2.44 \times 10^5 \mathrm{Nm}^2$ and mass per unit length ρA = 29.44 kg/m. As shown in **Figure 9**, damage was simulated by a designed crack-depth (a/H = 0.09, 0.27, 0.45) for each damage case (CL1,CL2,CL3) and located at 0.89m(x/L=0.248) from the left edge. The first two modal responses of these structures were obtained by the 3D finite elements models from the Ref.[32]. The 3D finite element model, with totally 28,512 block elements (288 elements

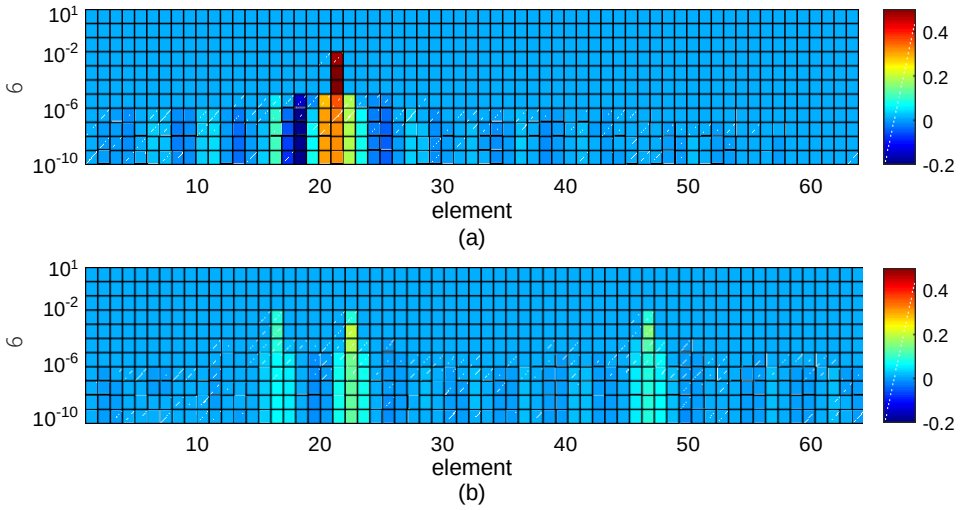

Figure 5 Change in *EI* with different values of regularization parameter λ: (a)D1 (b)D2

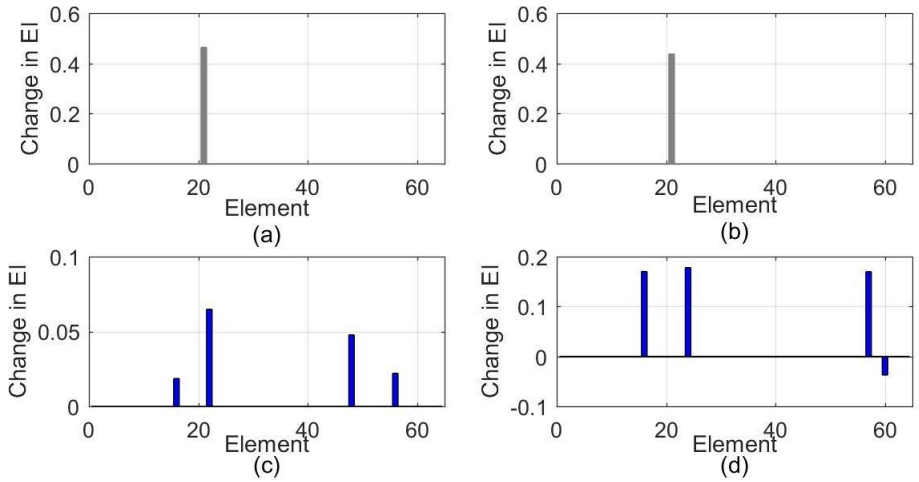

Figure 6 (a) damage identification result for D1 with 3% noise; (b) damage identification result for D1 with 5% noise; (c) damage identification result for D2 with 3% noise; (d) damage identification result for D2 with 5% noise

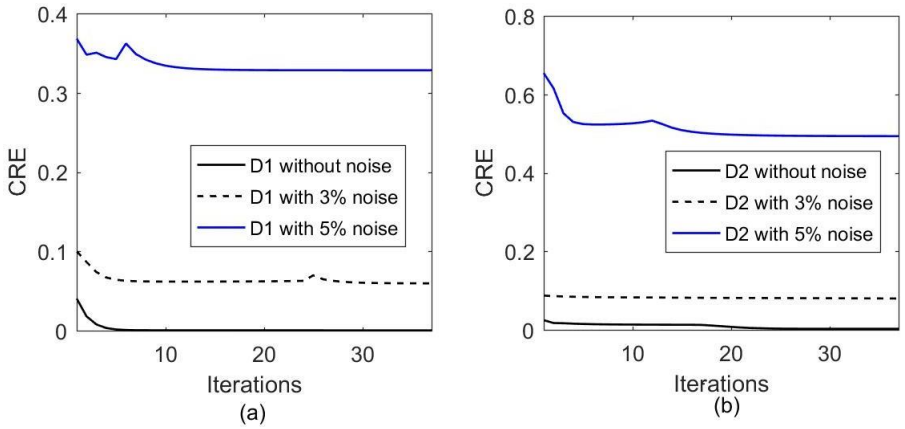

Figure 7 CRE vs iterations: (a)D1;(b)D2

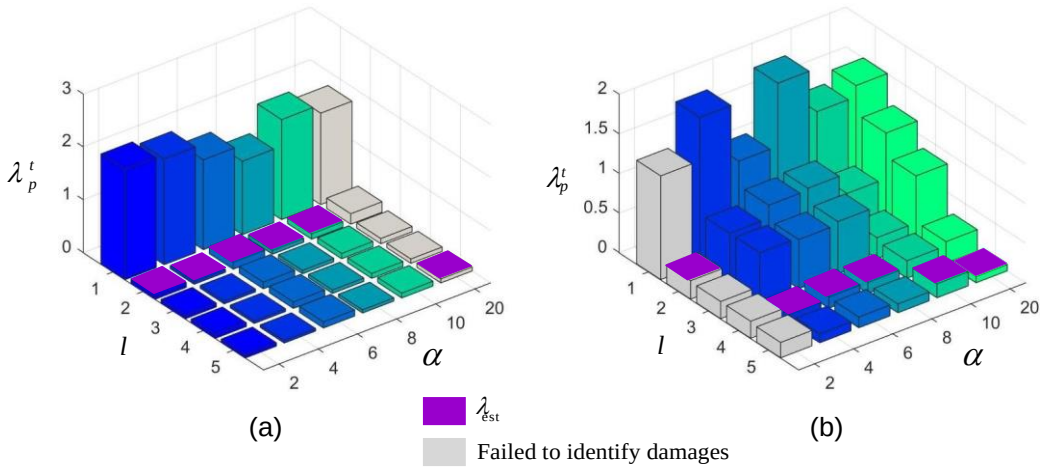

Figure 8 Adaptive choice of α (a)D1;(b)D2

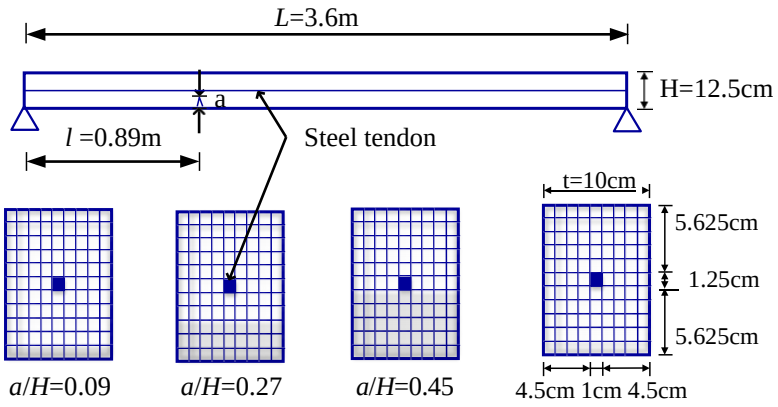

Figure 9 3D finite element model with different damage severities for modal responses

Table 1 Measured frequencies and modal displacements of cracked simply supported beam

Case-order	Frequency(Hz)	x/L=0.1	0.2	0.3	0.4	0.5	0.6	0.7	0.8	0.9
CL1-1	11.162	0.632	1.182	1.585	1.843	1.927	1.836	1.576	1.169	0.614
CL1-2	43.857	1.168	1.839	1.766	1.035	0.055	-1.118	-1.808	-1.847	-1.154
CL2-1	11.019	0.635	1.208	1.598	1.842	1.912	1.820	1.557	1.159	0.612
CL2-2	42.701	1.170	1.839	1.766	0.959	-0.122	-1.146	-1.805	-1.821	-1.139
CL3-1	10.746	0.664	1.254	1.640	1.85	1.901	1.791	1.531	1.134	0.604
CL3-2	40.825	1.170	1.909	1.737	0.879	-0.209	-1.220	-1.813	-1.777	-1.094

along the length of the beam) used for the modal analysis, was generated using the commercial software ANSYS and damage was inflicted by reducing the stiffness of the appropriate elements. The vibration amplitude was measured at nine equally spaced positions, each of which was 36cm between two adjacent locations.

For the sake of convenience, Damage Index is introduced to represent the scaled damage in the beam, i.e.

$$\text{Damage Index}_p = k_p^{\text{damage}}/k_{0p} \tag{22}$$

where k_p^{damage} is the damaged stiffness and k_{0p} is the stiffness before damaged in element p.

In Ref.[32], a mode-shape-based damage detection method based on the sensitivity approach, using the Euler-Bernoulli beam model with 288 elements of equal size, was used to identify the damage, while the model for damage detection in the min-CRE approach consists of 50 elements.

Damage identification results for each damage case obtained by the min-CRE approach as well as the sensitivity approach in Ref.[32] are summarized in **Table 2**. It is shown that the min-CRE approach could give nearly the same results for damage localization as well as damage extent assessment in CL2 (middle damage case) and even superior results in CL3 (large damage

Table 2 Damage identification of simply supported beam compared to the results[32]

Damage case -method	Damage Index (FE model)	Predicted Damage Range Elements(Location)	Most Probable Element(Location)	Damage Index (Identified)	λ_{est}
CL1-CRE	0.76	6-10(0.1-0.2)	10(0.20)	0.973	0.230
CL1-reference[32]	0.76	55-81(0.191-0.280)	67(0.233)	0.926	\
CL2-CRE	0.41	11-15(0.2-0.3)	13(0.26)	0.62	0.300
CL2-reference[32]	0.41	55-80(0.191-0.277)	67(0.233)	0.636	\
CL3-CRE	0.22	11-15(0.2-0.3)	11(0.22)	0.29	0.466
CL3-reference[32]	0.22	55-81(0.191-0.277)	67(0.233)	0.491	\

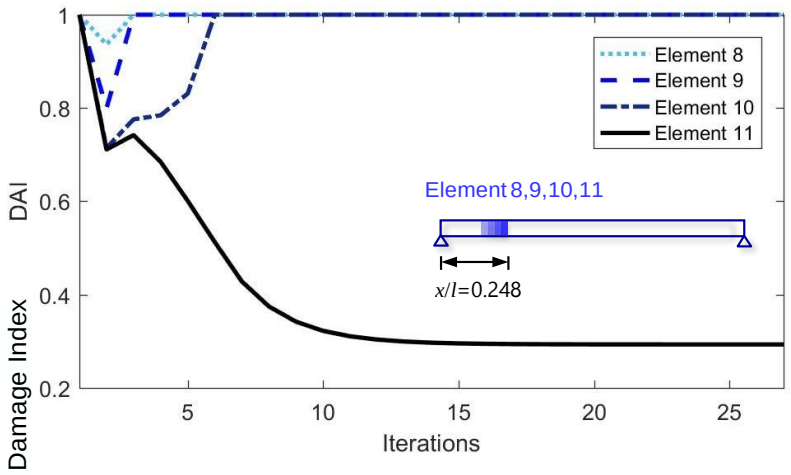

Figure 10 Convergence of Damage Index for simply supported beam in CL3

case) when compared with the results in Ref.[32]. The accuracy of the damage localization by the present approach was evaluated by measuring the localization error, ranged from 5% to 19% and the accuracy of damage severity is from 21% to 33%. For CL1 (small damage case), the identified results obtained by the present min-CRE approach are reasonable and slightly less satisfactory than the results by the sensitivity approach. This is mostly caused by the fact that under small damage, the difference/error between the displacement finite element model and the force finite element modal may be in the same level with the discrepancy of the derived modal data between the damaged and undamaged structures.

To visualize the convergence of the min-CRE approach for the large damage case, detailed results on the damage index of the most probable damaged element 11 and its nearest elements 8-10 at each iteration step, are given in **Figure 10**. Obviously, all the quantities converge within

27 iterations verifying the convergence of the proposed two-step substitution algorithm even for the large damage case.

4.3 A plane frame structure

A plane frame structure[19] as shown in **Figure 11** is to be studied to demonstrate the robustness of the proposed sparse regularization technique. The axial displacement u_x, tension force N and the corresponding longitudinal inertial force f_t are additionally considered in this case. The damage parameter is set to be $\mathcal{K} = E(x)$ instead of $EI(x)$. The height and width of the frame are $H = L \times 2 = 8\text{m}$ and $L = 4\text{m}$, respectively, with the inertial moment for planar bending $I = 5 \times 10^{-9}\text{m}^4$ and cross-sectional area $A = 1 \times 10^{-7}\text{m}^4$. For the undamaged frame, the mass density of the material is $\rho = 10^7\text{kg/m}^3$ and the Young's modulus is $E = 2 \times 10^8\text{N/m}^2$. The plane frame consists of 24 Euler-Bernoulli beam elements with 24 nodes, each with three degree of freedom. The vibration amplitude measurement locations and corresponding direction are also illustrated in **Figure 11** and the measured modal displacements are normalized with respect to the maximum vibration amplitude. Herein, the Young's modulus of each element is identified and no damage pattern is needed to be assumed before the identification process, which is different from Ref.[19].

Two damage cases are considered: damages were enforced by reducing the Young's modulus E to 25% in element 1 and 75% in element 9 in case D1 and to 85% in element 1 and 85% in element 9 in case D2. According to Ref.[19], damage case D1 with large stiffness differences for close elements was selected based on the experience due to its hard identifiability. The first three modes and their frequencies are used herein and all modes are equally weighted. The normal distribution noise described in Equation (21) is used and noises of level 2%, 5% and 10% (SNR=17dB, 13dB and 10dB) are considered in this example. Again, noise for natural frequencies are not considered herein.

As shown in **Figure 12**(a) and **Figure 13**(a), good identification performance is achieved when there is no noise. The optimal regularization parameter λ_{est} is 3.4×10^{-4} and 1.1×10^{-4}. To get a better picture for the cases with noise, statistical analysis was performed. Mean values and standard deviations of damage index over 100 Monte Carlo trials with different levels of noise are presented in **Figure 12**(b)(c)(d) and **Figure 13**(b)(c)(d). The mean of the optimal regularization parameters is 1.7×10^{-3}, 2.3×10^{-3} and 6.0×10^{-3} for D1 and 1.3×10^{-3}, 2.7×10^{-3} and 5.5×10^{-3} for D2. Satisfactory identification results are observed even under the noise level 10%.

Figure 14 compares the results obtained by the min-CRE approach in D1 with the identification results in Ref.[19], where a sensitivity-based approach with Tikhonov regularization was used. Obviously, the sparse-regularized min-CRE approach gives the best estimation of the

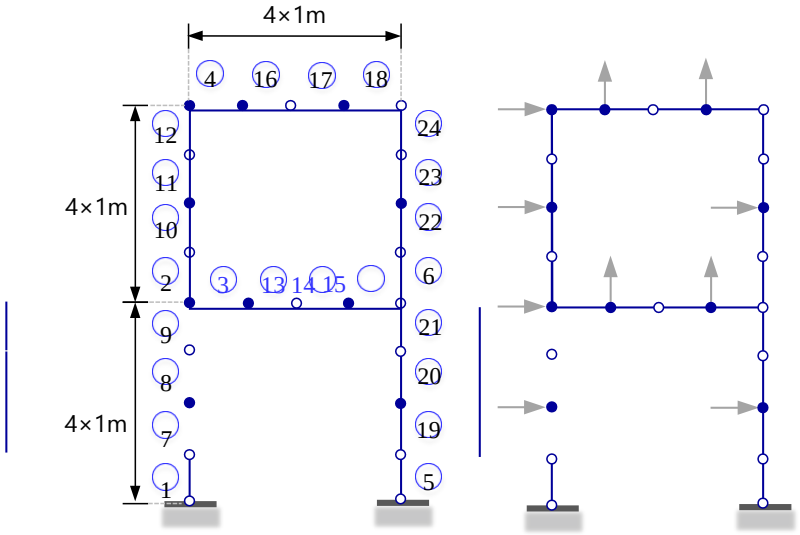

Figure 11 Model and measurement points of plane frame structure

damage parameters in terms of the mean values and standard deviations of the damage indices. The reason for different levels of standard deviation is possibly because some elements are more sensitive to perturbation errors than others. Moreover, it is clear that the sparse regularization greatly improves the identifiability and robustness of the min-CRE approach by comparing the results between **Figure 14**(b)(min-CRE approach without regularization) and (d)(min-CRE approach with regularization).

To visualize how the sparse-regularized min-CRE approach proceeds, the iterative procedure for the case of 5% noise is shown in **Figure 15**. Although it seems to take a little more steps to get the convergence, this approach would still be an efficient tool for structural damage identification.

5 Experimental verification

5.1 Crack identification in a cantilever beam

A single cracked cantilever beam as shown in **Figure 16** is adopted as the first experimental verification example. The crack is assumed to remain a continuum and the mechanical properties (stiffness EI in beam model or Young's modulus E in plane stress model) are modified to account for the effect of cracking, that is, the following models do not account for discontinuities in the topology of the FE mesh for this kind of general damage identification problem.

The length of the beam is L = 300mm with square cross-section $h \times d$ = 20mm × 20mm. The stiffness of beam is $k_0 = EI = 2.75 \times 10^3 \text{Nm}^2$ and the mass per unit length is taken

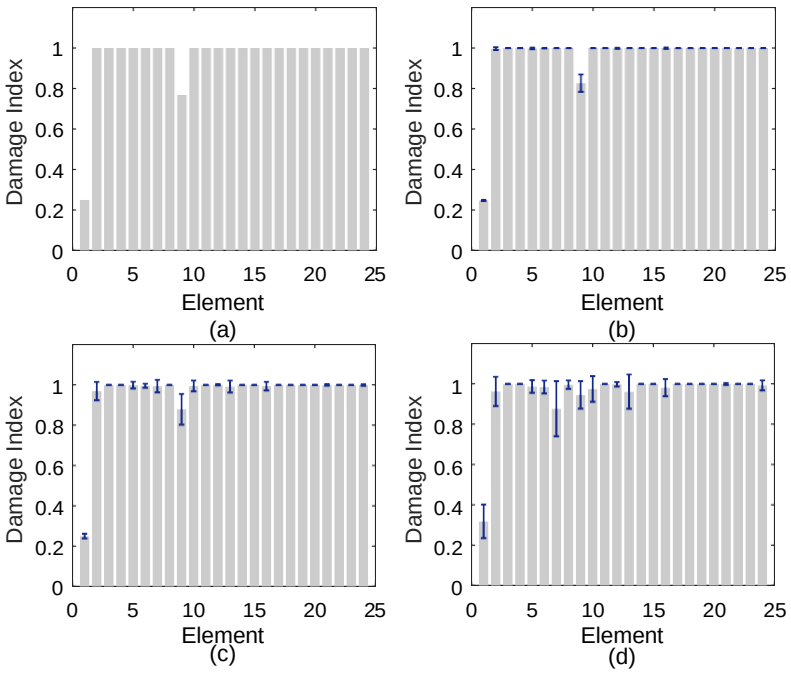

Figure 12 Mean values and standard deviations of Damage Index for: (a) no noise; (b) 2% noise; (c) 5% noise; (d) 10% noise in D1

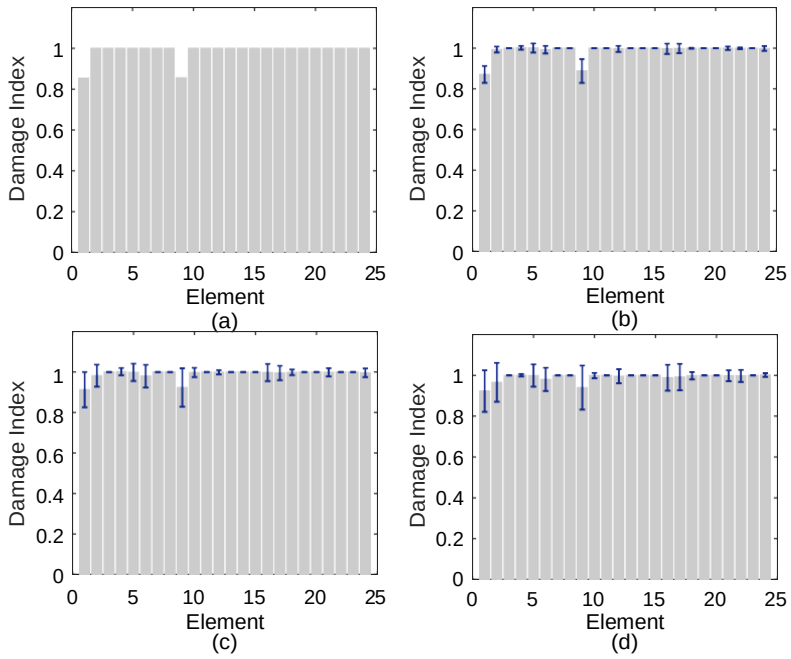

Figure 13 Mean values and standard deviations of Damage Index for: (a) no noise; (b) 2% noise; (c) 5% noise; (d) 10% noise in D2

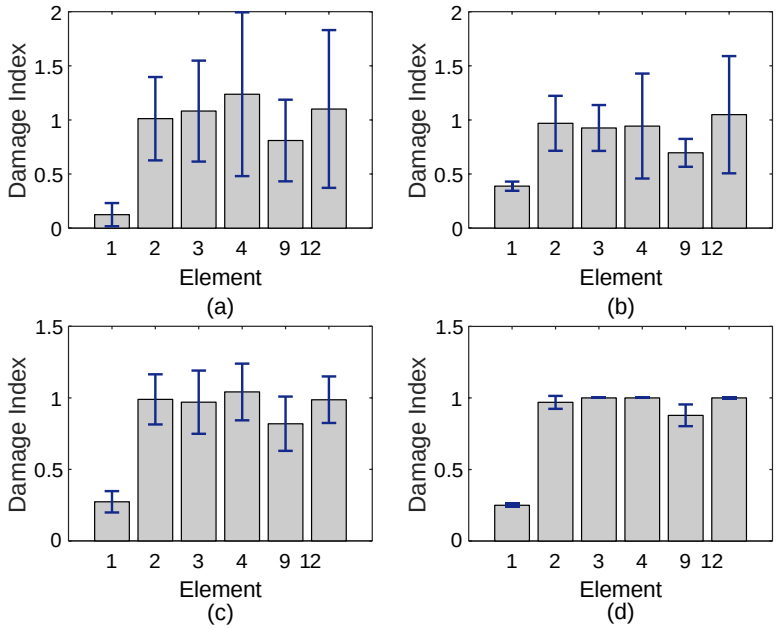

Figure 14 Identification results with 5% noise by: (a) reference[19] without regularization; (b) min-CRE without regularization;(c) reference[19] with regularization; (d) min-CRE with regularization

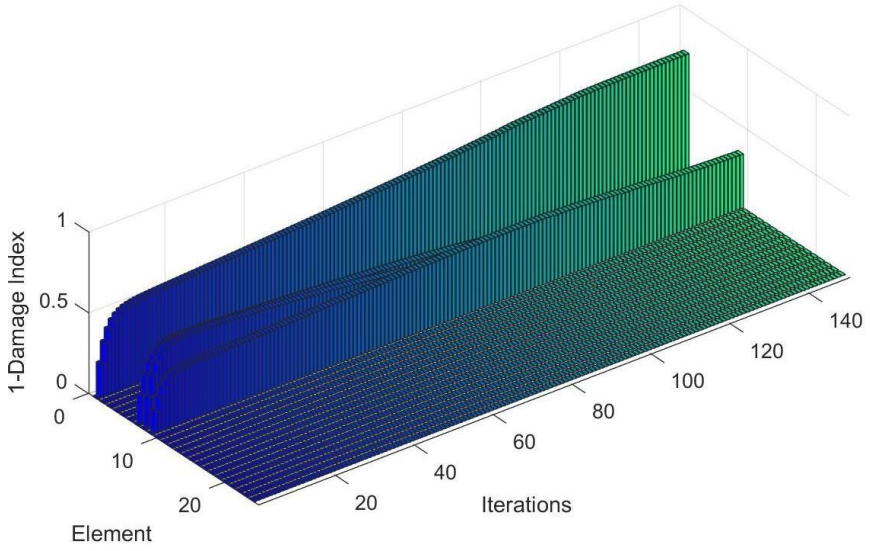

Figure 15 Damage identification procedure of plane frame structure

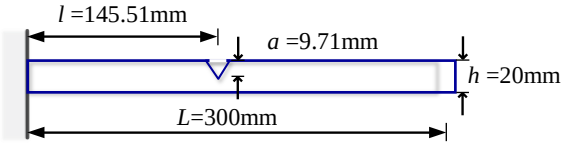

Figure 16 The cracked cantilever beam specimen

Table 3 Measured frequencies and modal displacements of cracked cantilever beam

Order	Frequency(Hz)	x/L=0.1	0.2	0.3	0.4	0.5	0.6	0.7	0.9	1.0
1	171	0.027	0.063	0.109	0.156	0.236	0.354	0.487	0.778	0.940
2	987	0.069	0.149	0.276	0.444	0.516	0.400	0.200	-0.455	-0.899
3	3034	0.033	0.103	0.221	0.288	0.011	-0.387	-0.498	-0.203	0.435

to be ρA = 3.12 kg/m. The crack is located at l = 145.51mm from the clamped end with depth a = 9.71mm. The crack was initiated with a thin saw-cut and propagated to the desired depth by fatigue loading. The crack depth was measured directly and verified with an ultrasonic detector for uniformity and actual depth. The measured natural frequencies and modal responses were obtained experimentally[33]. Electromagnetic vibrator, amplifier and accelerometer were utilized in the experiment. Harmonic excitation was applied and only one mode at a time was investigated. The signal generator could be tuned to the natural frequency of interest automatically by using a frequency hunting circuit.

The vibration amplitude was measured at the positions 30mm, 60mm, 90mm, 120mm, 150mm, 180mm, 210mm, 270mm and 300mm. The amplitude of motion at 240mm was not measured. The vibration signal was transferred to a vibration analyzer and a recorder to give plots of vibration amplitude versus frequency. The first three mode shapes were measured by using two calibrated accelerometers mounted on the beam. One accelerometer was kept at the clamped end of the beam to measure the mode amplitude. The data used in this case is summarized in **Table 3**. It should be noted that the modal displacements herein contain not only the measurement errors but also digitized process errors when extracted from the published paper[33] (see also the Ref.[34]).

By performing the two-step substitution algorithm in Section 3, the min-CRE approach for damage identification can be used. The optimal regularization parameter obtained by the threshold setting method is λ_{est} = 197.97. Well identification performance for the structure is achieved by the proposed sparse-regularized approach with comparision to the identification results in the Ref.[34] and detailed results are shown in **Figure 17**. In the Ref.[34], the same

frequencies and modal displacements data in **Table 3** were used and an algorithm was proposed considering changes in estimated constitutive properties of the finite element model with an output-error parameter estimation algorithm to localize the damage. Two models were used for damage detection in the Ref.[34]

- model A: structure modelled by 50 Bernoulli-Euler beam elements;
- model B: structure modelled by 60 two-dimensional plane stress square four-node elements without geometric defects (30 elements on the top row and 30 elements on the bottom row).

Accordingly, structure with 50 Bernoulli-Euler beam elements, compared with Model A in the reference and structure with 30 Bernoulli-Euler beam elements, compared with Model B are established for damage identification in the sparse-regularized min-CRE approach.

For the beam model case, although the crack was identified by model A in the Ref.[34], elements at other locations such as element 31 and 46 were also detected as damaged. The crack actually lied between element 22 and 24 and the results from the min-CRE approach clearly identify a range of elements 21-25. Model B in Ref.[34] offered a much better result than model A: elements 12-15 on the top row and 13-15 on the bottom row were detected as damages, while the beam model of the min-CRE approach again exhibits a very good identification performance: the crack lies between element 13 and 15, which are the exact damage locations. Obviously, the distributive stiffness is well identified with limited and incomplete experimental modal data by the sparse-regularized min-CRE approach.

5.2 Crack identification in a beam with two fixed ends

The proposed damage identification algorithm was also applied to an aluminum beam with two fixed ends[35] as shown in **Figure 18**. The parameters are set as follows: E = 70GPa, υ = 0.3 and $\rho = 2.7 \times 10^3 \mathrm{kg/m}^3$. A saw-cut damage was applied by cutting two cracks on the top and bottom surface of the intact beam with a depth of quarter of the total thickness of the beam for each crack. Experimental modal data were obtained by the impact excitation and only one accelerometer was employed at the center of the beam to measure the deflection response. Modal responses were attained through one line in the transfer function matrix. More details of this experiment could be found in Ref.[35]. The first three-order frequencies and mode shapes of the damaged beam are used herein (**Figure 18**). Based on the FEM computation from Ref.[35], the saw-cut damage could be simulated using 87.5% reduction of the bending stiffness in the ninth element.

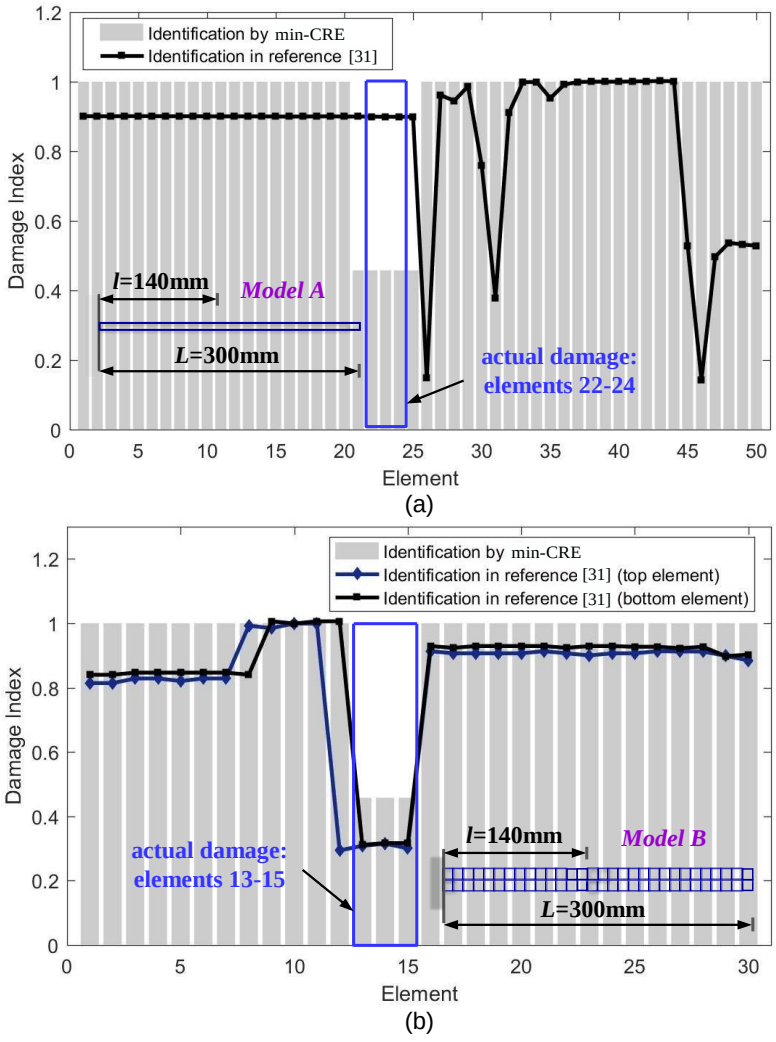

Figure 17 Identification results using sparse-regularized min-CRE approach compared to the results in Ref.[34] (model A and model B)

Two identification methods which are similar in concept to the best achievable eigenvector technique were proposed in Ref.[35]. The first (DDNKM) does not employ the analytical global stiffness and mass matrices completely; the second one (DDNK) uses the analytical global mass matrix only. These approaches first locate the damages using a special subspace rotation algorithm, and then identify the magnitude of damage using the quadratic programming technique.

By employing the first two orders of measured modal data, the identification results using DDNKM, DDNK and min-CRE approach are shown in **Figure 19**(a), (b) and (c) respectively. It can be found that the damaged element 9 can be detected very clearly from the min-CRE approach. The damage extent of the min-CRE approach is reasonable, although not as accurate as DDNK. The reason that the proposed algorithm exhibits such strong capability in damage location is that the sparsity could extract the most important features from the measured information (the damage) while suppress the less important ones which seems to be introduced by the noise. The optimal regularization parameter obtained by the threshold setting method is $\lambda_{\text{est}} = 738.76$, suggesting a strong enforcement of sparsity and hence the identified damage extent is slightly biased. The same phenomenon could be seen from the case employing the first three orders of measured modal data (**Figure 20**). In this case, the sparse-regularized min-CRE approach offers a much better identification results than the other two methods in Ref.[35], no matter in regard to the assessment of the damage localization or the damage extent. However, compared with the results from the min-CRE approach based on the first two orders of measured modal data, no obvious improvement seems to be attained for this case. The reason is that the first two modes are already enough to detect the damage and higher level measured error may be invoked in the third mode. A relatively small weight coefficient is suggested to be chosen for the third mode in this situation as mentioned in Section 2.3.

For further comparison, the recently developed damage identification approach via sparse representation (SR) classification in Ref.[23] is also called to identify the damage in the beam. Note from the above analysis that using the first two modes have led to better identification results than using the first three modes and therefore, only the first two modes are adopted for damage identification by the SR approach herein. In doing so, two stages are involved:

- Stage 1. Identification of damage location

    1. Predefine damage classes of the beam (see **Figure 18**) with all possible damage locations and then, details are presented **Table 4**. For each damage class, get the first two incomplete mode shapes that correspond to the measured first two mode shapes. Then, collect the first two incomplete mode shapes of all damage classes to

form the reference matrix.

2. For each of the two measured mode shapes, use A_1 minimization to obtain the sparse solution. Then, calculate the recovery error of each damage class by referring to the definition in Ref.[23] and detailed results on the recovery error are displayed in **Figure 21**(a). Clearly, damage location at element 9 is well identified because the damage class with the smallest recovery error is in principle the desired one for the beam.

◦ Stage 2. Identification of damage extent

1. Predefine damage classes of the beam with predefined damage location at element 9 and all possible damage extents for which the details are listed in **Table 5**.
2. Repeat Stage 1 except that the predefined damage classes in **Table 5** is used and then, results on the recovery error under different damage extents are obtainable as depicted in **Figure 21**(b). Obviously, the damage extent of 70% is identified.

To conclude, damage location at element 9 of extent 70% has been well identified in the beam by the two-step SR approach in Ref.[23]. Comparing the identification results in Figure 19(c) by the proposed sparse-regularized min-CRE approach with the identification results by the two- step SR approach, both approaches have given rise to satisfactory identification of the damage: damage location at element 9 is perfectly detected with almost no fictious damage locations while damage extent around 0.7 is also reasonably identified. The good performance of both approaches shall be benefit from the sparsity assumption—sparsity of damage locations for the proposed sparse-regularized min-CRE approach and sparsity of damage classes for the two- step SR approach. Correspondingly, the importance of the sparsity in damage identification is recognized. It should be noticed that the SR approach is efficient and robust for both single and multiple damage cases, but it is found that this approach is incapable of identifying small damage with very limited sensors[23]. However, as is shown in the numerical example, the proposed sparse-regularized min-CRE approach can well identify small damages if the damage locations are scarce enough. In other words, in case when small damages occur at a single or scarce location, the proposed approach is recommended.

6 Conclusions

A modal-based damage identification approach by the minimum constitutive relation error (min-CRE) principle and the sparse regularization was proposed in this paper. To this end, a (sep-

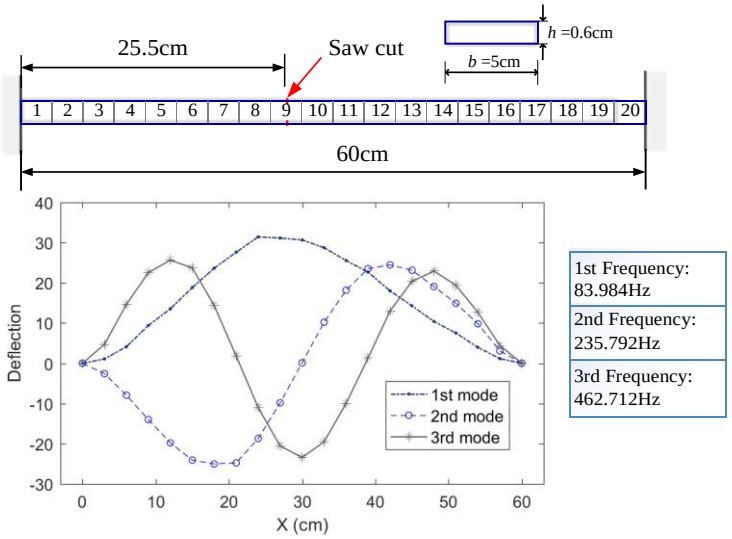

Figure 18 A beam with two fixed ends and its first three order measured modes (damaged)

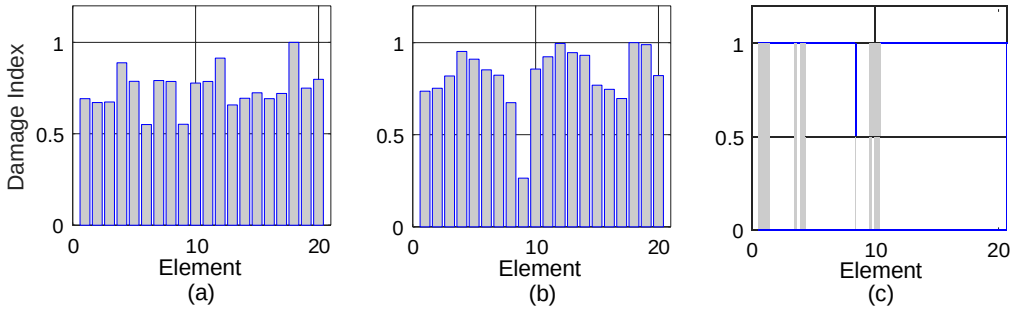

Figure 19 Identification results by employing the first two orders of measured modal data: (a)DDNKM (b)DDNK (c)sparse-regularized min-CRE

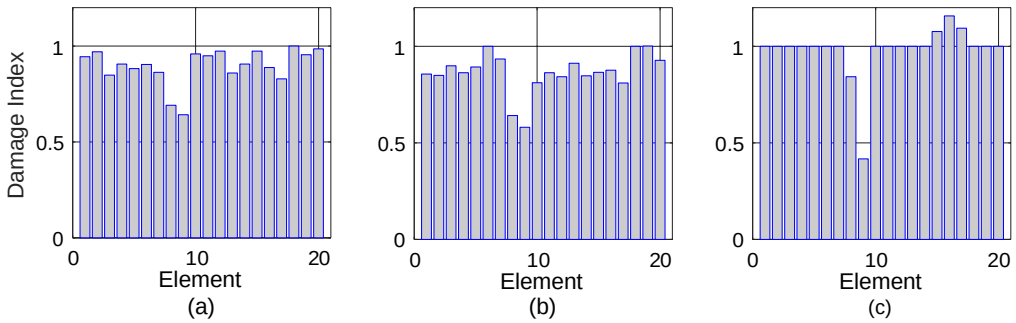

Figure 20 Identification results by employing the first three orders of measured modal data: (a)DDNKM (b)DDNK (c)sparse-regularized min-CRE

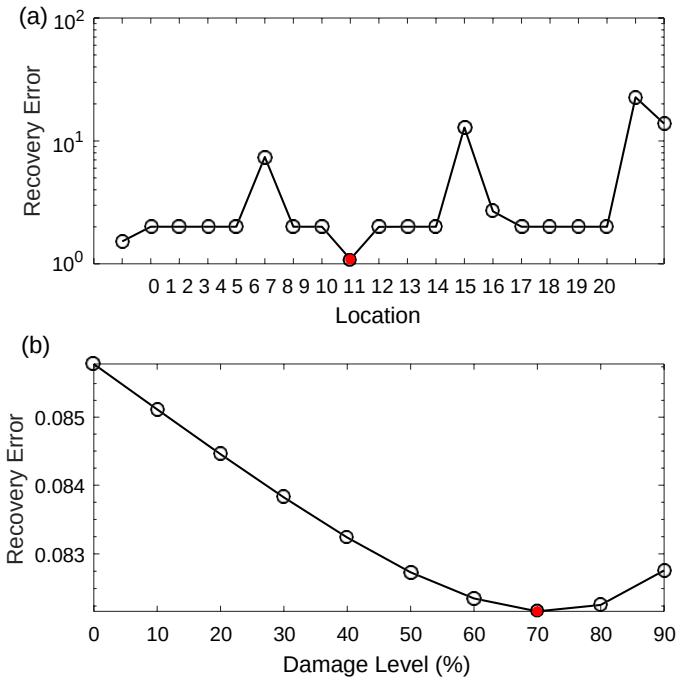

Figure 21 Identification results by SR of (a) damage location and (b) damage extent

Table 4 Predefined damage classes of the beam for Stage 1

Class	1	2	3	...	19	20
Damage location	Element 1	Element 2	Element 3	...	Element 19	Element 20
Damage extent	50%	50%	50%	...	50%	50%
Obtained incomplete mode shapes	$\Phi_1 \in R^{19\times 2}$	$\Phi_2 \in R^{19\times 2}$	$\Phi_3 \in R^{19\times 2}$	...	$\Phi_{19} \in R^{19\times 2}$	$\Phi_{20} \in R^{19\times 2}$
Reference matrix	$\Psi_1 = [\Phi_1, \Phi_2, \cdots, \Phi_{19}, \Phi_{20}] \in R^{19\times 40}$					

Table 5 Predefined damage classes of the beam for Stage 2

Class	1	2	3	...	9	10
Damage location	Element 9	Element 9	Element 9	...	Element 9	Element 9
Damage extent	0%	10%	20%	...	80%	90%
Obtained incomplete mode shapes	$\Phi_1 \in R^{19\times 2}$	$\Phi_2 \in R^{19\times 2}$	$\Phi_3 \in R^{19\times 2}$	...	$\Phi_9 \in R^{19\times 2}$	$\Phi_{10} \in R^{19\times 2}$
Reference matrix	$\Psi_2 = [\Phi_1, \Phi_2, \cdots, \Phi_9, \Phi_{10}] \in R^{19\times 20}$					

arately) convex objective function, also known as the CRE, to measure the residual of the constitutive equations connecting between the admissible stress field and the admissible displacement field has been established and the sparse regularization has been enforced to enhance the robustness of the damage identification with insufficient modal data. A two-step substitution algorithm was then applied to practically get the solution and a simple strategy for automatically selecting the regularization parameter was presented. Results show that:

1. The present threshold setting method to get the regularization parameter is effective.
2. The present sparse-regularized min-CRE approach can give good identification results of the damage locations and severities for damage with relatively few damage locations, while for damage with multiple damage locations, identification of the damage location is still satisfactory.
3. The sparse regularization indeed enhances the robustness of the damage identification procedure with insufficient modal data and measurement noise.
4. The present damage identification approach performs well in both numerical and experimental tests.

Thus, it is believed that the proposed approach can serve as an effective tool for practical structural damage identification using incomplete modal data. Also note that the present approach is based on a clear physics model of the structure. In practice, both Neumann and Dirichlet boundary conditions could be less reliable. Hence, an identification strategy enabling to take into account all the available information and capable to deal with different reliability levels of information should be considered in the future research.

Appendix: Finite element formulation for the UMF step

A finite dimensional space $\mathfrak{I}_0^h \subset \mathfrak{I}_0$ and $\mathcal{U}_0^h \subset \mathcal{U}_0$ are constructed at first with h denoting the characteristic mesh size. For each mode, the nodal forces (Q_i, M_i) and displacements (θ_i, u_i) at an arbitrary node i are naturally selected as the basic DOFs to solve the admissible force solution and displacement solution, respectively. Then, for an arbitrary element e with two nodes i, j whose coordinates are $x_i < x_j$, the following approximation (Q_h, M_h) and (θ_h, u_h) are adopted for the force and displacement finite element computation,

$$\begin{aligned} M_h^e &= (H_1 \quad H_2 \quad H_3 \quad H_4)\, \boldsymbol{F}^e,\ \boldsymbol{F}^e = \left[Q_i, M_i, Q_j, M_j\right] \\ u_h^e &= (H_1 \quad H_2 \quad H_3 \quad H_4)\, \boldsymbol{W}^e,\ \boldsymbol{W}^e = \left[\theta_i, u_i, \theta_j, u_j\right] \end{aligned} \tag{1}$$

where the superscript e denotes the restriction into element e and the polynomial interpolation

functions H_1, H_2, H_3, H_4 are of the following forms,

$$\begin{cases} H_1(\xi) = \frac{1}{2}(\xi+2)(\xi-1)^2, H_2(\xi) = \frac{1}{4}(\xi+1)(\xi-1)^2\frac{h^e}{2}, \\ H_3(\xi) = \frac{1}{2}(2-\xi)(\xi+1)^2, H_4(\xi) = \frac{1}{4}(\xi-1)(\xi+1)^2\frac{h^e}{2}, \\ h^e = x_j - x_i, \xi = \frac{2(x-x_i)}{h^e} - 1. \end{cases} \tag{2}$$

For brevity, the total finite element approximation is designated as

$$M_h = \hat{\boldsymbol{\Phi}}\boldsymbol{F}, u_h = \boldsymbol{\Phi}\boldsymbol{W} \tag{3}$$

where $\boldsymbol{F}$ and $\boldsymbol{W}$ collect all the DOFs with *a priori* satisfaction of the Neumann boundary condition and Dirichelet boundary condition. Using the finite element approximation (3), the discrete formulation of equations (12) and (13) is obtained

$$\begin{aligned} &\begin{pmatrix} \boldsymbol{A}_0 & -\boldsymbol{C}_0 \\ -\boldsymbol{C}_0^T & \boldsymbol{B}_0 \end{pmatrix}\begin{pmatrix} \boldsymbol{F} \\ \boldsymbol{W} \end{pmatrix} = \begin{pmatrix} a \\ b \end{pmatrix} \\ &\boldsymbol{A} = \int_X \left\{ r\frac{\hat{\boldsymbol{\Phi}}^T\hat{\boldsymbol{\Phi}}}{EI} + (1-r)\frac{\hat{\boldsymbol{\Phi}}^{T}{}''\hat{\boldsymbol{\Phi}}''}{\omega^2\rho A} \right\} dx \\ &\boldsymbol{B} = \int_X \{ r\boldsymbol{\Phi}^{T}{}''EI\boldsymbol{\Phi}'' + (1-r)\boldsymbol{\Phi}^T\omega^2\rho A\boldsymbol{\Phi} \} dx + \boldsymbol{P} \\ &\boldsymbol{P} \text{ a digonal matrix with } \boldsymbol{P}(k,k) = \begin{cases} A_k, k \in \wp \\ 0, k \notin \wp \end{cases} \\ &\boldsymbol{C} = \int_X \hat{\boldsymbol{\Phi}}^{T}{}''\boldsymbol{\Phi} dx \\ &a = 0, b = p, p(k) = \begin{cases} A_k\hat{u}_k, k \in \wp \\ 0, k \notin \wp \end{cases} \end{aligned} \tag{4}$$

where $\boldsymbol{A}_0$,$\boldsymbol{B}_0$ and $\boldsymbol{C}_0$ are the reduced forms of $\boldsymbol{A}$,$\boldsymbol{B}$ and $\boldsymbol{C}$ after applying the homogeneous boundary conditions.

Acknowledgement

The present research was performed under the support of the MEXT scholarship of Japan.

References

[1] Wei Fan and Pizhong Qiao. Vibration-based damage identification methods: a review and comparative study. *Structural Health Monitoring*, 10(1):83–111, 2011.

[2] ZY Shi, SS Law, and LM Zhang. Structural damage localization from modal strain energy change. *Journal of Sound and Vibration*, 218(5):825–844, 1998.

[3] Pillip Cornwell, Scott W Doebling, and Charles R Farrar. Application of the strain energy damage detection method to plate-like structures. *Journal of Sound and Vibration*, 224(2): 359–374, 1999.

[4] ZY Shi, SS Law, and LM Zhang. Structural damage detection from modal strain energy change. *Journal of Engineering Mechanics-ASCE*, 126(12):1216–1223, 2000.

[5] Parviz Moradipour, Tommy HT Chan, and Chaminda Gallage. An improved modal strain energy method for structural damage detection, 2d simulation. *Structural Engineering and Mechanics*, 54(1):105–119, 2015.

[6] Robert Y Liang, Jialou Hu, and Fred Choy. Theoretical study of crack-induced eigenfrequency changes on beam structures. *Journal of Engineering Mechanics-ASCE*, 118(2): 384–396, 1992.

[7] Charbel Farhat and Francois M Hemez. Updating finite element dynamic models using an element-by-element sensitivity methodology. *AIAA Journal*, 31(9), 1993.

[8] Hua-Peng Chen and Than Soe Maung. Regularised finite element model updating using measured incomplete modal data. *Journal of Sound and Vibration*, 333(21):5566–5582, 2014.

[9] Giuseppe Geymonat and Stéphane Pagano. Identification of mechanical properties by displacement field measurement: a variational approach. *Meccanica*, 38(5):535–545, 2003.

[10] Béatrice Faverjon and J-J Sinou. Robust damage assessment of multiple cracks based on the frequency response function and the constitutive relation error updating method. *Journal of Sound and Vibration*, 312(4):821–837, 2008.

[11] Eric Florentin and Gilles Lubineau. Using constitutive equation gap method for identification of elastic material parameters: technical insights and illustrations. *International Journal on Interactive Design and Manufacturing*, 5(4):227–234, 2011.

[12] Pierre Ladeveze and Dominique Leguillon. Error estimate procedure in the finite element method and applications. *SIAM Journal on Numerical Analysis*, 20(3):485–509, 1983.

[13] Jia Guo and Izuru Takewaki. Minimum constitutive relation error based static identification of beams using force method. In *Journal of Physics: Conference Series*, volume 842, page 012026. IOP Publishing, 2017.

[14] Pierre Feissel and Olivier Allix. Modified constitutive relation error identification strategy for transient dynamics with corrupted data: The elastic case. *Computer Methods in Applied Mechanics and Engineering*, 196(13):1968–1983, 2007.

[15] Benoˆıt Blaysat, E Florentin, Gilles Lubineau, and Ali Moussawi. A dissipation gap method for full-field measurement-based identification of elasto-plastic material parameters. *International Journal for Numerical Methods in Engineering*, 91(7):685–704, 2012.

[16] Marc Bonnet and Andrei Constantinescu. Inverse problems in elasticity. *Inverse Problems*, 21(2):R1, 2005.

[17] Biswanath Banerjee, Timothy F Walsh, Wilkins Aquino, and Marc Bonnet. Large scale parameter estimation problems in frequency-domain elastodynamics using an error in constitutive equation functional. *Computer Methods in Applied Mechanics and Engineering*, 253:60–72, 2013.

[18] Michael Friswell and John E Mottershead. *Finite element model updating in structural dynamics*, volume 38. Springer Science & Business Media, 2013.

[19] Benedikt Weber, Patrick Paultre, and Jean Proulx. Structural damage detection using nonlinear parameter identification with tikhonov regularization. *Structural Control and Health Monitoring*, 14(3):406–427, 2007.

[20] B Titurus and MI Friswell. Regularization in model updating. *International Journal for Numerical Methods in Engineering*, 75(4):440–478, 2008.

[21] CD Zhang and YL Xu. Comparative studies on damage identification with tikhonov regularization and sparse regularization. *Structural Control and Health Monitoring*, 23(3): 560–579, 2016.

[22] Emmanuel J Candes, Michael B Wakin, and Stephen P Boyd. Enhancing sparsity by reweighted A_1 minimization. *Journal of Fourier Analysis and Applications*, 14(5):877–905, 2008.

[23] Yongchao Yang and Satish Nagarajaiah. Structural damage identification via a combination of blind feature extraction and sparse representation classification. *Mechanical Systems and Signal Processing*, 45(1):1–23, 2014.

[24] Satish Nagarajaiah and Yongchao Yang. Modeling and harnessing sparse and low-rank data structure: a new paradigm for structural dynamics, identification, damage detection, and health monitoring. *Structural Control and Health Monitoring*, 24(1), 2017.

[25] Yongchao Yang and Satish Nagarajaiah. Output-only modal identification with limited sensors using sparse component analysis. *Journal of Sound and Vibration*, 332(19):4741–4765, 2013.

[26] Yongchao Yang and Satish Nagarajaiah. Output-only modal identification by compressed sensing: Non-uniform low-rate random sampling. *Mechanical Systems and Signal Processing*, 56:15–34, 2015.

[27] Ying Wang and Hong Hao. Damage identification scheme based on compressive sensing. *Journal of Computing in Civil Engineering-ASCE*, 29(2):04014037, 2013.

[28] Chun Zhang, Jie-Zhong Huang, Gu-Quan Song, and Lin Chen. Structural damage identification by extended kalman filter with A_1-norm regularization scheme. *Structural Control and Health Monitoring*, page e1999, 2017. URL http://dx.doi.org/10.1002/stc.1999.

[29] Mark Schmidt. Least squares optimization with l1-norm regularization. *CS542B Project Report*, pages 14–18, 2005.

[30] Mee Young Park and Trevor Hastie. L1-regularization path algorithm for generalized linear models. *Journal of the Royal Statistical Society: Series B (Statistical Methodology)*, 69(4): 659–677, 2007.

[31] M Saiidi, B Douglas, and S Feng. Prestress force effect on vibration frequency of concrete bridges. *Journal of Structural Engineering-ASCE*, 120(7):2233–2241, 1994.

[32] Jeong-Tae Kim, Yeon-Sun Ryu, Hyun-Man Cho, and Norris Stubbs. Damage identification in beam-type structures: frequency-based method vs mode-shape-based method. *Engineering Structures*, 25(1):57–67, 2003.

[33] PF Rizos, N Aspragathos, and AD Dimarogonas. Identification of crack location and magnitude in a cantilever beam from the vibration modes. *Journal of Sound and Vibration*, 138(3):381–388, 1990.

[34] KD Hjelmstad and S Shin. Crack identification in a cantilever beam from modal response. *Journal of Sound and Vibration*, 198(5):527–545, 1996.

[35] N Hu, X Wang, H Fukunaga, ZH Yao, HX Zhang, and ZS Wu. Damage assessment of structures using modal test data. *International Journal of solids and structures*, 38(18): 3111–3126, 2001.